processes

MDPI

*Article*

# Vapor Overproduction Condition Monitoring in a Liquid–Vapor Ejector

**Serhii Sharapov [1], Jana Mižáková [2,*], Danylo Husiev [1], Vitalii Panchenko [3], Vitalii Ivanov [4], Ivan Pavlenko [5] and Kamil Židek [2]**

1 Department of Technical Thermophysics, Faculty of Technical Systems and Energy Efficient Technologies, Sumy State University, 2, Rymskogo-Korsakova St., 40007 Sumy, Ukraine
2 Department of Industrial Engineering and Informatics, Faculty of Manufacturing Technologies, Technical University of Kosice, Bayerova 1, 080 01 Prešov, Slovakia
3 Department of Applied Hydroaeromechanics, Faculty of Technical Systems and Energy Efficient Technologies, Sumy State University, 2, Rymskogo-Korsakova St., 40007 Sumy, Ukraine
4 Department of Manufacturing Engineering, Machines and Tools, Faculty of Technical Systems and Energy Efficient Technologies, Sumy State University, 2, Rymskogo-Korsakova St., 40007 Sumy, Ukraine
5 Department of Computational Mechanics named after V. Martsynkovskyy, Faculty of Technical Systems and Energy Efficient Technologies, Sumy State University, 2, Rymskogo-Korsakova St., 40007 Sumy, Ukraine
* Correspondence: jana.mizakova@tuke.sk; Tel.: +421-556026409

**Abstract:** We consider the influence of vapor content in the mixed flow leaving a liquid-vapor ejector on the energy efficiency of a vacuum unit. As shown by numerical studies of liquid-vapor ejectors, this issue is important as vapor overproduction, which accompanies the process of secondary flow ejection, directly impacts the efficiency of the working process of both the liquid-vapor ejector and the vacuum unit as a whole. The greater the degree of vapor overproduction, the greater the load on the vapor phase of the separator, which is part of the vacuum unit. In addition, the liquid phase must be returned to the cycle to ensure the constancy of the mass flow rate of the working fluid of the primary flow. Our numerical study results revealed the rational value of the degree of vapor overproduction at which the efficiency of the liquid–vapor ejector was maximized, and the amount of additional working fluid that needed to enter the cycle of the vacuum unit was minimal. Experimental condition monitoring studies on the liquid–vapor ejector were carried out on plane-parallel transparent models with different flow path geometries. Through experimental studies, we confirmed and adjusted the values of the achievable efficiency of the working process of a liquid–vapor ejector, depending on the degree of vapor overproduction. Using a comparative analysis of liquid–vapor ejectors with different flow path geometries, differences were revealed in their working processes, which consisted of the degree of completion of the mixing of the working media of primary and secondary flows. To determine the feasibility of using liquid–vapor ejectors with different flow path geometries, exergy analysis was performed, resulting in achievable efficiency indicators.

**Keywords:** liquid–vapor ejector; degree of vapor overproduction; experimental study; interchangeable geometry; energy efficiency; vacuum unit



**Citation:** Sharapov, S.; Mižáková, J.; Husiev, D.; Panchenko, V.; Ivanov, V.; Pavlenko, I.; Židek, K. Vapor Overproduction Condition Monitoring in a Liquid–Vapor Ejector. *Processes* **2022**, *10*, 2383. https://doi.org/10.3390/pr10112383

Academic Editor: Udo Fritsching

Received: 19 September 2022
Accepted: 10 November 2022
Published: 13 November 2022



## 1. Introduction

In the modern world, the main problem facing all industries is ensuring energy efficiency and environmental protection. This is why, for various industries, it is necessary to develop installations and systems that are energy efficient and do not harm the environment [1,2].

Technological processes implemented at below atmospheric pressures [3–5] are becoming widely used. One of the new types of devices used in such systems is a liquid–vapor ejector (LVE), which operates on the principle of jet thermal compression. Water that is not heated to saturation is used as the primary stream. The process of boiling occurs when

the active flow flows out of the nozzle. Further pumping of passive flow also occurs, which can be the vapor phase of almost any substance or mixture. Water is a cheap and environmentally friendly product to be used as the working substance of a primary flow, and its use in such systems is innovative and promising.

The efficiency of such an apparatus and a vacuum unit depends on the completeness of the mixing of the primary and secondary flows and achieving the required parameters for the mixed flow at the LVE outlet. One of the main indicators is the degree of vapor overproduction. This parameter determines the amount of steam that must be returned to the cycle. It is evaluated as the difference between the amount of steam removed from the separator as a vapor phase and the amount of the ejected passive flow.

This investigation is relevant to increasing the energy efficiency of existing technological systems and creating new, more efficient and environmentally safe schemes. This is because liquid–steam ejectors are a better alternative to existing steam jet ejectors. They do not require the external generation of working steam, which simplifies the process and does not require additional energy consumption.

Simultaneously, in order to evaluate the expected effect of a new apparatus, it is necessary to perform numerical and experimental studies of liquid–vapor ejectors with different flow path geometries. This would enable the implementation of the most rational and constructive solution.

### *1.1. Literature Review and Problem Statement*

Recent European and world studies have been devoted to exploring the operation of two-phase jet devices on different refrigerants or carbon dioxide [6–9]. Although they have significant advantages over single-phase devices, they have been studied due to their complex working process [10,11]. The main disadvantage of two-phase jet devices is the cost of the working medium (refrigerant) and issues of safety and environmental friendliness.

Recently, an increasing number of studies have suggested the use of water or water vapor, as in steam jet ejectors, as the working fluid of the primary flow [12–14]. However, in steam jet ejectors, steam generation takes place in external steam generators. This requires additional energy consumption and reduces the overall efficiency. In addition, water can have negative properties, including the formation of scale, which is inevitable under such working process conditions. This can be simply solved; the authors of [15] propose using ethers and aqueous solutions that have neutral properties and do not lead to interaction with a secondary flow at the chemical level.

Study of the geometry and design features of the flow path of two-phase jet devices are presented in [16–18]. The efficiency of the working process, both in the apparatus itself and in the whole system, directly depending on its parameters. As noted above, the workflow of two-phase jet devices is quite complex, which does not allow for unifying their development and production. Each device is developed for a specific purpose and a certain degree of pressure increase [19,20].

In this study, we investigated the influence of the flow path geometry and degree of steam overproduction in the mixed flow at the outlet of the liquid–vapor ejector on the efficiency of the entire operating process.

### *1.2. The Aim and Objectives of the Research*

The aim of this research is to evaluate the influence of the vapor overproduction value in the mixed flow leaving the liquid–vapor ejector with different flow path geometry on the efficiency of the working process of the vacuum unit.

To achieve this aim, the following objectives were formulated:

- Perform a numerical study of a liquid–vapor ejector with different geometries of the flow path with exact parameters for the working fluid of the primary flow at the LVE inlet and calculate the degree of vapor overproduction for each of the options;

- Conduct an experimental study of a liquid–vapor ejector with different geometries of the flow path with exact parameters of the working fluid of the primary flow at the LVE inlet and calculate the degree of vapor overproduction for each of the options;
- Carry out an exergy analysis of a liquid–vapor ejector with different flow path geometries and determine achievable performance indicators of the LVE and its corresponding vacuum unit.

## 2. Materials and Methods

In the following section, we describe the selection of operating parameters for condition monitoring and the numerical and experimental methods used to study the liquid–vapor ejector as part of a vacuum unit.

### *2.1. Initial Data and Design Schemes*

The initial data for numerical modeling and experimental research were chosen for the operation of a vacuum unit as part of a plant's vacuum cooling system for biodiesel fuel production [21,22].

Water was used as the working substance of the primary flow. At the inlet to the motive nozzle, it had the following parameters: pressure $p_{01}$ = 0.4 MPa, temperature $t_{01}$ = 135 °C, and mass flow $m_p$ = 0.4918 kg/s.

For the working substance of the secondary flow, water vapor was assessed, which had a pressure $p_{02}$ = 0.02 MPa at the inlet to the receiving chamber. The secondary flow temperature corresponded to the saturation temperature at the corresponding pressure. The mass flow rate $m_s$ was variable and depended on the injection ratio for each LVE with the corresponding geometry.

At the LVE outlet, there was a flow of a two-phase vapor droplet fine structure with a mass flow rate of the mixed flow, which is the sum of the flow rates of the primary and secondary flows. The pressure and temperature of the final flow depended on the geometrical and operating parameters of the flow part of the ejector. According to the study's goals, LVEs with different flow path geometries were considered, which differed in the geometric shape of the mixing chamber and in the presence or absence of a diffuser (Figure 1).

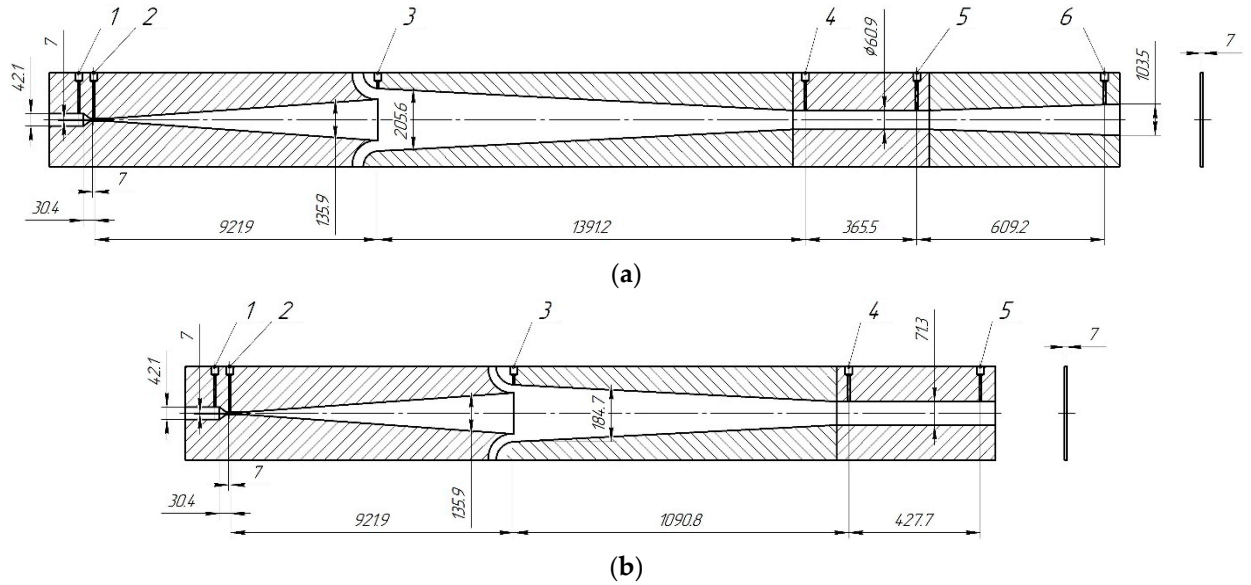


**Figure 1.** *Cont.*

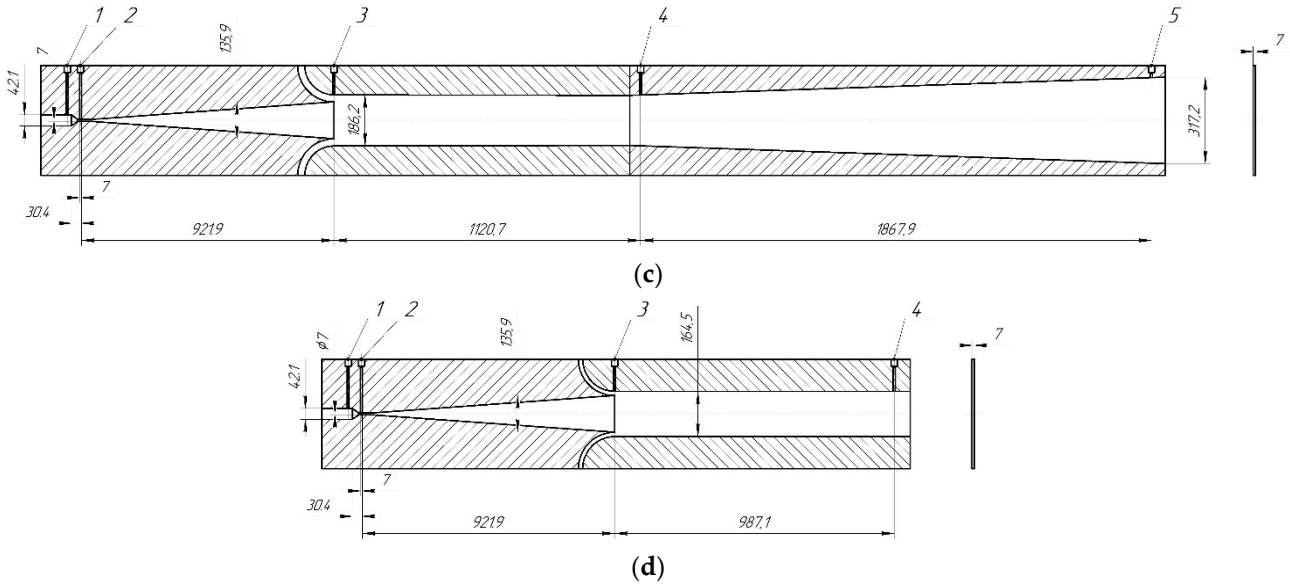


**Figure 1.** Design schemes of the liquid–vapor ejector with different geometry of the flow part (dimensions in mm): (**a**) with a conical mixing chamber and diffuser; (**b**) with a conical mixing chamber without a diffuser; (**c**) with a cylindrical mixing chamber and diffuser; and (**d**) with a cylindrical mixing chamber without a diffuser; 1–6 are places of pressure measurements.

### *2.2. Mathematical Model for Calculating the Working Process of a Liquid–Vapor Ejector*

To calculate the averaged parameters along the length of the flow path and total characteristics of the LVE, the system of equations of one-dimensional adiabatic motion in the quasi-equilibrium thermodynamic approximation was used for the selected boundaries of the considered flow section:

- The equation of state of a thermally metastable vapor-droplet medium

$$v = v_{liq}\left(t_{liq}\right) + x \cdot \left[v_{st}(p) - v_{liq}\left(t_{liq}\right)\right] d\left[\frac{w(z) \cdot F(z)}{v}\right] = 0 \quad (1)$$

- Mass conservation equation (taking into account the phase transition)

$$dx = \chi(z) \cdot \left[\frac{v}{w(z)}\right] dz \quad (2)$$

- Total enthalpy equation (1st law of thermodynamics)

$$d\left\{h_{liq}\left(t_{liq}\right) + x \cdot \left[h_{st}(p) - h_{liq}\left(t_{liq}\right)\right] + \frac{w^2(z)}{2}\right\} = 0 \quad (3)$$

- Momentum conservation equation

$$d\left[\frac{w^2(z) \cdot F(z)}{v}\right] = -F(z)dp - \tau_w \cdot \prod(z)dz \quad (4)$$

- Entropy production equation (2nd law of thermodynamics)

$$d\left\{s_{liq}\left(t_{liq}\right) + x \cdot \left[s_{st}(p) - s_{liq}\left(t_{liq}\right)\right]\right\} = \delta s_{diss} > 0 \quad (5)$$

- The equation of contact stresses arising on the wall

$$\tau_w = \left(\frac{\xi}{4}\right)^2 \cdot \frac{w^2(z)}{2 \cdot v}, \quad (6)$$

where $v$ is the specific volume of a particle of the $i$-th distribution group [m$^3$/kg]; $t$ is the temperature of the particle of the $i$-th distribution group (deg.); $w$ is the average particle flow velocity (m/s); $F$ is the area of the channel through which the particles of the $i$-th distribution group pass (m$^2$); $z$ is the dimensionless longitudinal coordinate; $\chi$—the mass moisture content (kg/kg]) $h$ is the enthalpy of a particle of the $i$ distribution group (J/kg); $\tau_w$ is the shear stress on the channel wall (Pa); $P$ is the perimeter of the channel through which particles of the $i$-th distribution group pass (m), $s$ is the entropy of a particle of the $i$-th distribution group (J/(kg·K); the index "*liq*" is the parameter in the liquid state; and index "*st*" is the parameter in the vapor state. The system of Equations (1)–(6) includes thermodynamic parameters (e.g., temperature and pressure) that evaluated parameters directly depend on (e.g., entropy, enthalpy, and specific volume). These values are determined from thermodynamic diagrams. Pressure varies in a range of 0.35–0.45 MPa, and the temperature range is 128–143 °C. Operating parameters (e.g., flow velocity, mass flow of secondary flow, and mass vapor content) vary in a very wide range, from subsonic values (inlet section) of the active flow nozzle to supersonic values (outlet section). At the outlet from the ejector, its value is 110–250 m/s.

The flow in the mixing chamber and ejector's inlet is subcritical. It significantly reduces energy losses when mixing active and passive currents. It also increases the efficiency of the whole process.

The value of the flow rate of the active stream is determined by calculations from the continuity equation. It ranges from 0.45 to 0.51 kg/s. The value of the mass flow rate of the passive flow is also a calculated value. However, it is a result of direct measurement of the volumetric flow rate using a flow meter.

The values of all measured and calculated parameters depend on the chosen design of the ejector (Figure 1).

Having solved the system of Equations (1)–(6) with the assumptions adopted in work, it is possible to obtain a formula for calculating the mass vapor content in the mixed flow of the finely dispersed structure of a two-phase vapor-droplet, which at the LVE outlet:

$$x_4 = \frac{h_4 - h_{4\,liq}}{r_4}, \quad (7)$$

where $h_4$ is the enthalpy of the mixed flow at the LVE outlet [J/kg] and $r_4$ is the specific heat of vaporization of the mixed flow at the LVE outlet [J/kg].

In the process of ejection of the secondary flow, which will be saturated water vapor, the two flows will be mixed. At the LVE outlet, there is a flow of a two-phase vapor droplet fine structure. The mixed mass flow rate ($m_t$) is the sum of the primary ($m_p$) and secondary ($m_s$) flows:

$$m_t = m_p + m_s. \quad (8)$$

During the separation process, most of the flow will be condensed and sent back to the operating cycle of the vacuum unit, and the non-condensed part ($m_{loss}$) will be removed as a vapor phase from the cycle. To keep the mass flow rate of the primary flow, and thus all cycle parameters constant, it is necessary to constantly return an additional mass of liquid to the cycle:

$$m_p = m_s + m_{loss}. \quad (9)$$

Substituting (8) into (9) and performing the transformation, we obtain a formula for determining the degree of vapor overproduction in the LVE working process. Its value will determine how much liquid must be returned to the cycle to maintain material balance:

$$\psi_4 = 1 + \frac{m_{loss}}{m_s}. \quad (10)$$

In a dimensionless form, the formula for determining the degree of vapor overproduction will look like

$$\psi_4 = \frac{x_4 \cdot (1+u)}{u}, \quad (11)$$

where u is the injection coefficient determined by the formula

$$u = \frac{m_s}{m_p}. \quad (12)$$

*2.3. Experimental Bench for Studying the Liquid–Vapor Ejector as Part of a Vacuum Unit*

The experimental bench for condition monitoring and LVE studies in vacuum mode (Figure 2) consists of an ejector, 1 and two heating tanks, 2 and 18, for heating water and auxiliary communications, pipelines, and fittings.

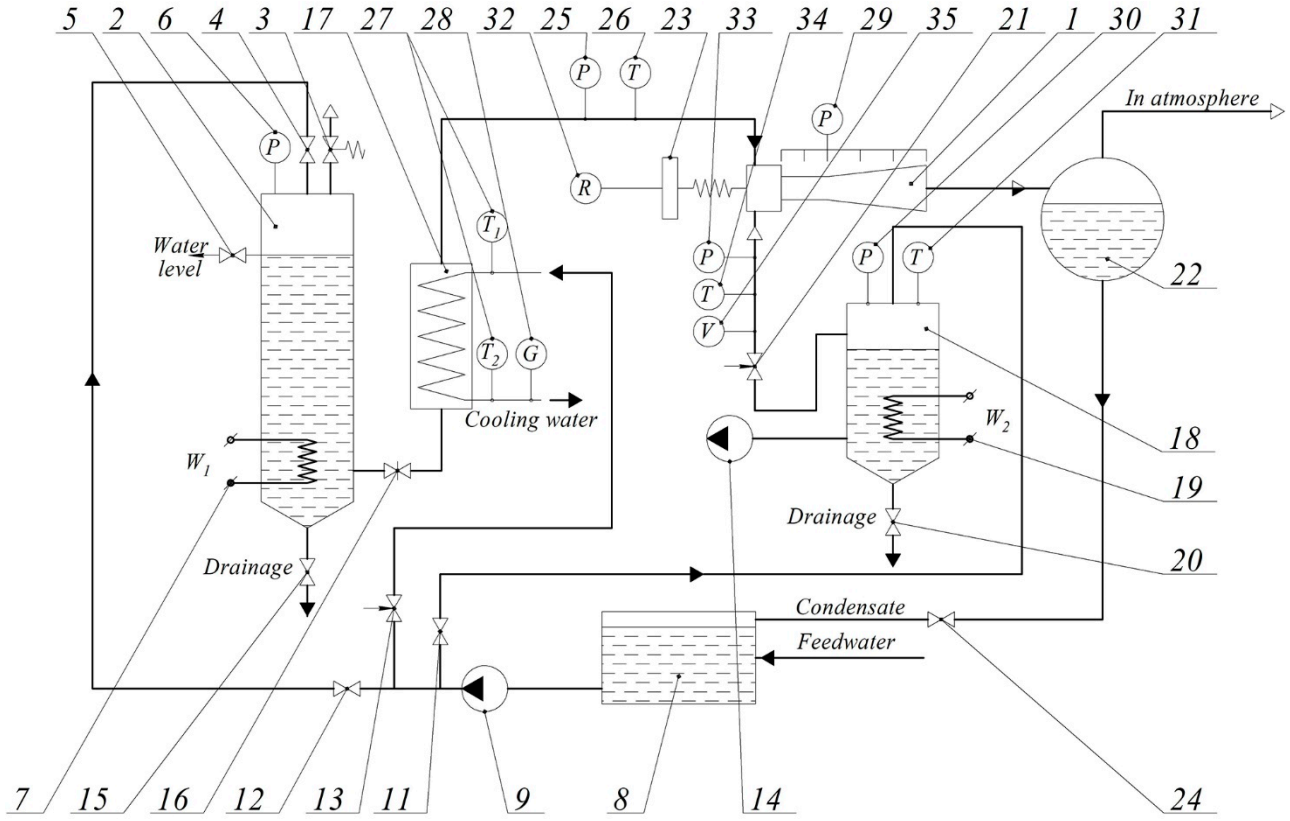


(**a**)

**Figure 2.** *Cont.*

(**b**)

**Figure 2.** The (**a**) design scheme and (**b**) photo of the experimental bench for research of liquid–vapor ejector as part of a vacuum unit: 1—LVE; 2, 18—heating container; 3—safety valve; 4, 5, 11, 12, 15, 20, 24—shut-off valve; 6, 25, 29—pressure gauge; 7, 19—block of heating elements; 8—water tank; 9—circulation pump; 13, 16, 21—control valve; 14—liquid ring vacuum pump; 17—heat exchanger of the "pipe in pipe" type; 22—separator; 23—digital scales; 26, 27, 31, 34—digital multimeter; 28—mass flow meter; 30, 33—vacuum gauge; and 35—volume flow meter.

When testing LVE in vacuum mode, the working fluid of the primary flow is supplied from tank 8 with the help of pump 9 to heating tank 2. Shut-off valves 4 and 12 stop the working fluid supply to the heating tank after filling it. The liquid level in the heating tank is controlled by valve 5. Then, the working fluid is heated by heater 7. The pressure in the tank is controlled by pressure gauge 6. Safety valve 3 is used for emergency pressure relief when the permissible value is exceeded. Discharge into the drain is carried out using valve 15.

After heating and reaching the required pressure that is equal to saturation pressure, the working fluid is fed through a tube-in-pipe heat exchanger 17 into the motive nozzle of LVE. The fluid flow is regulated by valve 16. Cooling water for the heat exchanger is supplied from tank 8. Water is circulated through the heat exchanger using pump 9. Shut-off valves 11 and 12 are used to open or close the cooling water supply to the pumps. The cooling water supply is adjusted using the control valve 13.

In the section from heating tank 2 to the motive nozzle, the following parameters are monitored: pressure—by pressure gauge 25, temperatures—by thermocouples with digital multimeters 26 and 27, and the mass flow of cooling water—by mass flow meter 28.

The secondary flow working fluid is supplied from tank 8 with the help of pump 9 to heating tank 18, which is heated by heating element 19. Stop valve 11 serves to stop the working fluid supply to the heating tank after it is filled. The vacuum value in heating tank 18 is provided by liquid ring vacuum pump 14 and is controlled by vacuum gauge 30. A thermocouple measures the temperature in heating tank 18 with digital multimeter 31. Discharge into the drain is carried out using valve 20.

Then, the vapor is fed into the receiving chamber of the secondary LVE flow. Its flow rate is regulated by valve 21. In the section from heating tank 18 to the fitting for

supplying it to the receiving chamber of the secondary LVE flow, the following parameters are controlled: vacuum value—with vacuum gauge 33, temperature—with a thermocouple with digital multimeter 34, volume flow—with flow meter 35.

After leaving the diffuser, the mixed flow enters separator 22, where it is separated into vapor and liquid phases. The vapor phase is discharged into the environment through the pipeline, and the liquid phase is drained through the pipelines into tank 8, from which it is pumped out by pump 9 to fill the heating tanks 2 and 18 or cool the working fluid of the primary flow in heat exchanger 17. Shut-off valve 24 works for the liquid phase from the separator. When studying the parameters of the working vapor jet, digital scales 23 were used to measure the momentum (reaction force).

The experimental LVE model (Figure 3) was made plane-parallel flat and had a flow path width of 7 mm, made of organic glass (polymethyl methacrylate).

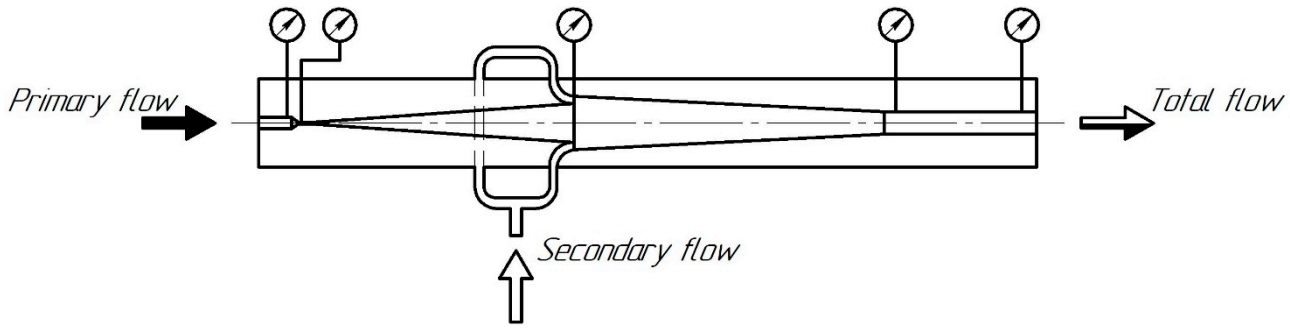


**Figure 3.** General view of the plane-parallel LVE model (with conical mixing chamber without diffuser).

The Mastech MT-838 digital multimeter and TR-01A thermocouple used for temperature measurement had an average systematic error of <1.5% in determining the absolute discharge pressure. The maximum error of temperature measurement by Chromel-Copel thermocouples, complete with a class 0.4 multimeter, did not exceed 1 °C. The maximum error in measuring mass costs, according to calibration tests, was 3%. Class 0.4 standard pressure gauges measured static pressure [23].

As a result of this study, we obtained the distribution of pressures and velocities of the working fluid of primary and secondary flows in the flow part of the LVE. The measurement error did not exceed 5%, with a confidence level of 0.95, which is acceptable for technical experiments. In another work [24], a similar measurement accuracy was achieved.

The velocity of working fluid at specific points was indirectly determined by measuring the nozzle's pressure, jet pulsation, and geometrical parameters.

### *2.4. Exergy Method for Analyzing a Vacuum Unit Based on a Liquid–Vapor Ejector*

The authors used the exergy thermodynamic analysis method to assess the effect of vapor overproduction in a liquid–vapor ejector on its efficiency. It was proposed by J. Tsatsaronis in [25,26]. It is a modern tool for evaluating the effectiveness of thermomechanical systems. It simplifies the determination of the total loss of work produced and expended due to the irreversibility of processes in the system under consideration. The main criterion for assessing the perfection of the system is the exergy efficiency ($\varepsilon_{ex}$), determined by the formula

$$\varepsilon_{ex} = 1 - \frac{summary\ losses}{expended\ energy}. \quad (13)$$

For the "liquid–vapor ejector + separator" system (Figure 4), the formula for the exergy efficiency can be written according to [27], as:

$$\varepsilon_{ex\ LVE+S} = \frac{E_{4\ st} - E_{02}}{E_{01} - E_{4\ liq}} = \psi_4 \cdot \frac{\dot{m}_s \cdot (e_{4\ st} - e_{02})}{\dot{m}_p \cdot \left(e_{01} - e_{4\ liq}\right)} \quad (14)$$

where $E_{01}$ and $E_{02}$ represent the exergy at the LVE inlet of the primary flow and secondary flow (saturated vapor), respectively; $E_{4\ liq}$ and $E_{4\ st}$ represent the exergy at the outlet of the liquid and vapor phase separator, respectively; $e_{01}$ and $e_{02}$ represent the specific exergy at the LVE inlet of the primary flow and secondary flow (saturated vapor), respectively; and $e_{4\ liq}$ and $e_{4\ st}$ represent the specific exergy at the liquid and vapor phase separator outlet, respectively.

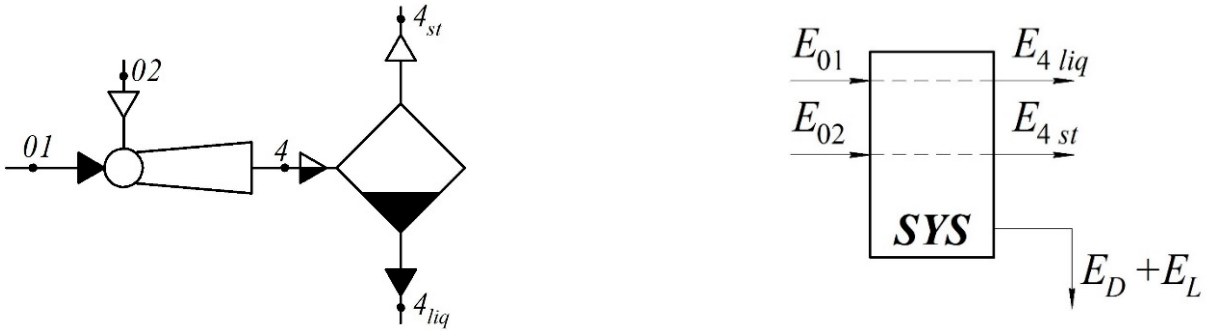


(**a**) (**b**)

**Figure 4.** (**a**) "LVE + separator" system diagram and (**b**) scheme of exergy transformations: $E_D + E_L$—destruction and losses of exergy.

After exergy transformations of Equation (14), taking into account formula (11), there is

$$\varepsilon_{ex\ LVE+S} = \psi_4 \cdot \frac{u \cdot (e_{4\ st} - e_{02})}{e_{01} - e_{4\ liq}}. \tag{15}$$

Similar to [27], the exergy efficiency for the vacuum unit system can be written as (Figure 5):

$$\varepsilon_{ex\ VU} = \frac{E_{4\ st} - E_{02}}{N_P + E_{Q_{H-E}}} = \frac{E_{4\ st} - E_{02}}{N_P + \left(E_{1_{H-E}} - E_{2_{H-E}}\right)}. \tag{16}$$

where $N_P$ is the power of the circulation pump; $E_{Q_{H-E}}$ is the exergy of the coolant flow in the heat exchanger; and $E_{1_{H-E}}$ and $E_{2_{H-E}}$ represent the exergy of the coolant flow at the inlet and outlet of the heat exchanger, respectively.

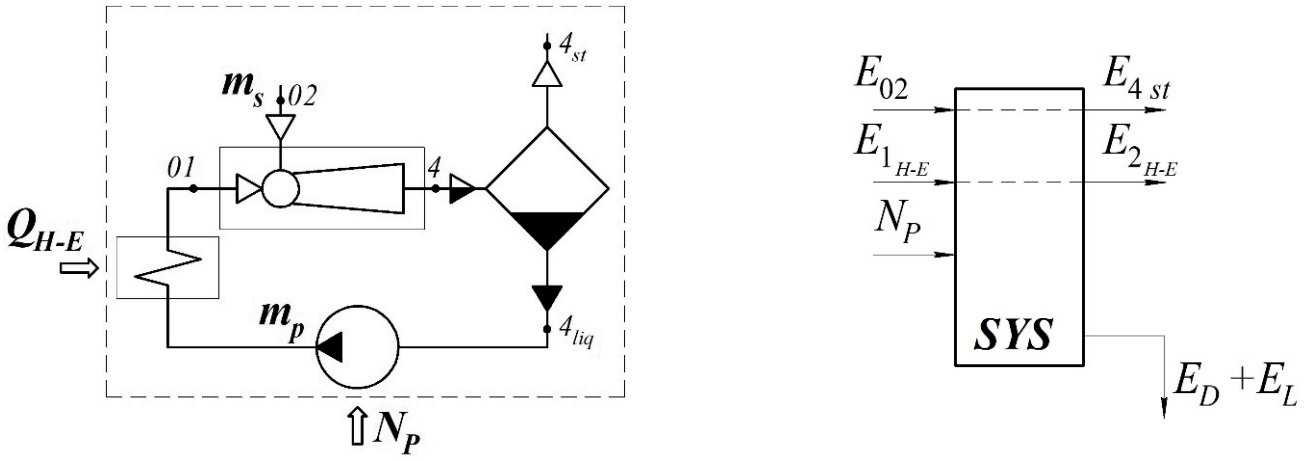


(**a**) (**b**)

**Figure 5.** (**a**) "LVE + separator" system diagram and (**b**) scheme of exergy transformations.

After exergy transformations, there is

$$\varepsilon_{ex\ VU} = \frac{m_s \cdot (e_{4\ st} - e_{02})}{N_P + m_{H-E} \cdot (e_{1_{H-E}} - e_{2_{H-E}})}. \quad (17)$$

where $m_{H-E}$ is the mass flow rate of the coolant in the heat exchanger and $e_{1_{H-E}}$ and $e_{2_{H-E}}$ represent the specific exergy of the coolant flow at the inlet and outlet of the heat exchanger, respectively.

### 2.5. Uncertainty Analysis

Table 1 presents all the values used during the study, the ways in which they were evaluated, and what accuracy they were given.

**Table 1.** Characteristics of the evaluated parameters.

| Parameter | Measurement | Calculation Error |
| --- | --- | --- |
| Pressure $p$, MPa | Direct measurements with pressure gauges and vacuum gauges. | Devices with different measurement ranges were used, depending on the pressure value in different ejector sections (Figure 1). The errors were in the range of 0.1–0.5%. |
| Temperature $t$, °C | Direct measurement with an electronic multimeter. | The total error of the thermocouple and multimeter for the temperature range of 100–150 °C was 1.2%. |
| Enthalpy $h$, J/kg | Tabular value | Half of the last digit (0.005%). |
| Entropy $s$, J/(kg·K) | Tabular value | Half of the last digit (0.005%). |
| Specific volume $v$, $m^3$/kg | Tabular value | Half of the last digit (0.005%). |
| Steam capacity $x$, kg/kg | Tabular value | Half of the last digit (0.005%). |
| Mass flow rate $m$, kg/s | For an active flow: direct measurement of the reactive force of the nozzle and calculation from the continuity equation. For a passive flow: measurement of volumetric flow rate with a flow meter. | The jet force of the nozzle was measured with an error of 1.5%. The total calculation error for components of the continuity equation was 1.6%. The error in determining the volumetric flow rate was 1%. The tabular value of the density had an error of 0.5%. The total error did not exceed 1.2%. |
| Velocity $v$, m/s | The estimated value depends on the consumption of active and passive flows. | Did not exceed 1.6%. |
| Injection ratio $u$ | Estimated value by formula (12) | Did not exceed 1.6%. |
| Specific exergy $e$, J/kg | Determined separately for liquid and steam phases as dependencies on the measured temperatures and pressures, as well as tabular values of enthalpy and density. | Did not exceed 1.4%. |

**Table 1.** *Cont.*

| Parameter | Measurement | Calculation Error |
|---|---|---|
| Exergy $E$, W | The estimated values are determined based on the specific exergy and mass flow rate. | Did not exceed 1.6%. |
| Exergy efficiency $\varepsilon_{ex}$ | Estimated value by formulas (15) and (17). | Did not exceed 1.6%. |

The LVE efficiency, according to the experiment results, is determined from the data of direct measurements and processing of experimental data.

The steam overproduction degree is determined by formula (11), based on direct and indirect measurements of the values presented in Table 1. Its total relative error is evaluated by the following formula:

$$\delta\psi_4 = b \cdot \sqrt{\left(\frac{\Delta P_4}{P_4}\right)^2 + \left(\frac{\Delta T_4}{T_4}\right)^2 + \left(\frac{\Delta x_4}{x_4}\right)^2 + \left(\frac{\Delta m_p}{m_p}\right)^2 + \left(\frac{\Delta m_s}{m_s}\right)^2}, \quad (18)$$

where $b$ is the coefficient that depends on the total number of measurements; $P_4$, $T_4$, and $x_4$ are the measured or calculated values of pressure, temperature, and mass vapor content in the mixed flow at the outlet of the ejector, respectively; $m_p$ and $m_s$ represent the calculated mass flow rates of active and passive flows, respectively; $\Delta P_4$, $\Delta T_4$, $\Delta x_4$, $\Delta m_p$, and $\Delta m_s$ represent values of absolute errors of measurement or calculation of the corresponding quantities.

According to expression (18), the total relative error of the steam overproduction degree is 1.65%.

## 3. Results

To verify the reliability of the results experimentally obtained by condition monitoring [28], the authors of the work performed additional mathematical modeling in the Ansys CFX Academic software package.

The system of Navier–Stokes equations for compressible media was used. The turbulence was considered using the k-ε model. Thus, a joint solution of the Navier–Stokes equations for time-averaged variables and additional equations to determine the pulsation components were used.

The Rayleigh–Plesset equation was also applied to determine the growth dynamics of steam bubbles. The mass transfer between the liquid and vapor phases was considered using the equations of evaporation and condensation.

The nozzle model created in Ansys CFX was axisymmetric. The calculation grid was automatically generated and consisted of approximately 50,000 cells. The mesh was compacted in places where the geometry of the flow part changed. Water, which boils in the diffuser part of the nozzle, was used as the working fluid of the active flow. Water vapor was used as the working fluid of the passive flow. The properties of the working fluids were taken from the Ansys CFX material database, according to the industry standard, IAPWS.

Input and output parameters are given in Section 2.1. The boundary conditions were defined as “Inlet” with “Volume Flow Rate”, “Wall” without roughness, and “Outlet” with the “Average Static Pressure”. Ambient pressure was considered equal to atmospheric pressure under normal conditions (101,325 Pa).

As a result of the comparison of numerical and experimental data, the average value of the absolute error did not exceed 1.5%.

Figure 6 shows a graph of the pressure distribution along the length of the flow path of the LVE with different geometry, following Figure 1.

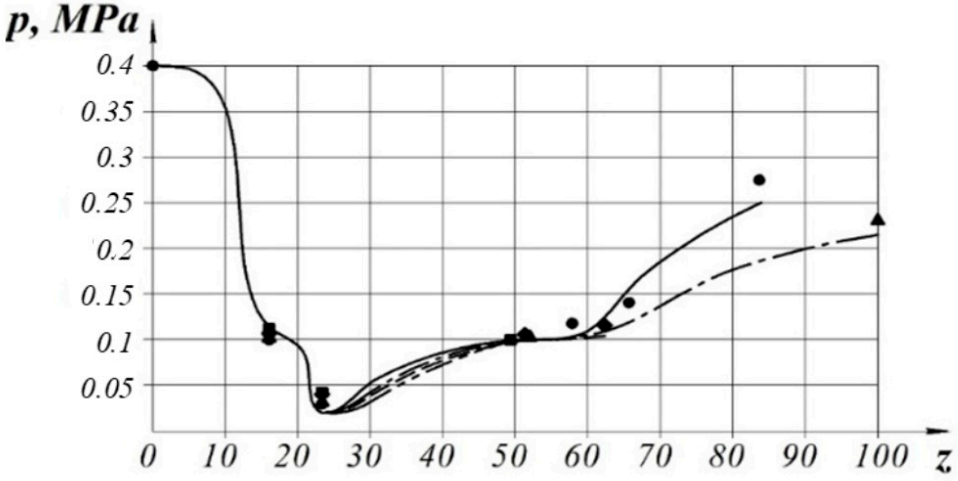


**Figure 6.** Pressure distribution along the length of the LVE flow path. Results of numerical research: ———for the design of the ejector presented on Figure 1a; - - - - —for the design of the ejector presented on Figure 1b; - · - · - —for the design of the ejector presented on Figure 1c; and - · - · - · - —for the design of the ejector presented on Figure 1d. Experimental data: ●—for the design of the ejector presented on Figure 1a; ◆—for the design of the ejector presented on Figure 1b; ▲—for the design of the ejector presented on Figure 1c; and ■—for the design of the ejector presented on Figure 1d.

From Figure 6, it can be seen that LVE with a cylindrical or conical mixing chamber without a diffuser at the outlet will have lower pressures at the level $p_4$ = 0.1–0.12 MPa. Accordingly, the degree of increase in the pressure of the secondary flow will be decreased, leading to an additional load on the circulation pump, which must be provided with pressure at the inlet to the LVE $p_{01}$ = 0.4 MPa.

For LVE with a cylindrical or conical mixing chamber and diffuser, $p_4$ = 0.22–0.25 MPa.

In addition, according to the results of the experimental studies and calculations using formulas (8) and (12), we can determine the injection coefficient for LVE without a diffuser as $u$ = 0.03–0.05 and with a diffuser as $u$ = 0.07–0.12. Thus, LVE with a diffuser pumps out a larger amount of secondary flow per unit of time, that is, an average of 37.5% greater productivity.

Figure 7 shows a graph of the distribution of mass content vapors along the length of the LVE flow path with different geometry, following Figure 1. It can be seen that in a LVE with a cylindrical or conical mixing chamber without a diffuser, the output will be much larger ($x_{4max}$ = 0.271) than in a LVE with a diffuser ($x_{4max}$ = 0.127). Having made calculations according to Formulas (7) and (11), it is possible to determine the degree of vapor overproduction. For LVE without a diffuser, it is $\psi_4$ = 1.517–2.273, and for LVE with a diffuser, $\psi_4$ = 1.118–1.426.

After carrying out experimental studies of a liquid–vapor ejector without a diffuser, and performing calculations of the steam overproduction degree by formula (10), the value of $m_{loss}$ was greater. Therefore, it is necessary to return more water to the cycle to ensure that the condition $m_p = const$ is met.

Figure 8 shows a generalized theoretical dependence of the degree of vapor overproduction and injection coefficient on the mass content of vapor in the secondary flow at the LVE inlet. It can be seen that, with an increase in the mass content of vapor in the secondary flow at the LVE inlet, the injection coefficient increases, but the overproduction of vapor in the working process decreases.

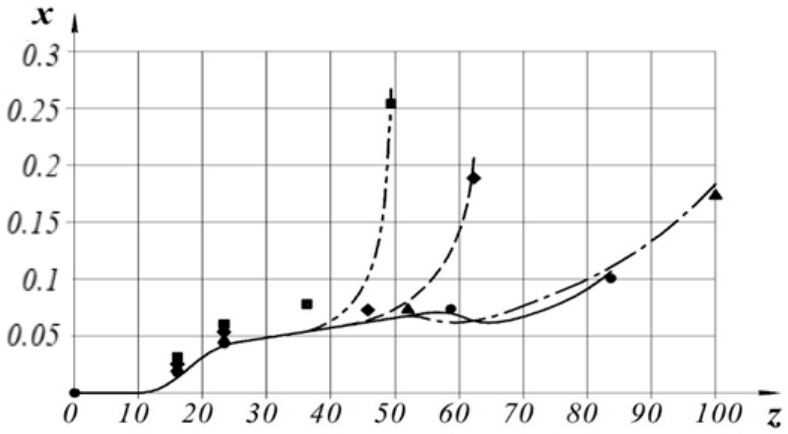


**Figure 7.** Distribution of mass content vapors along the length of the LVE flow path. Results of numerical research: ———for the design of the ejector presented on Figure 1a; - - - - —for the design of the ejector presented on Figure 1b; - · - · - —for the design of the ejector presented on Figure 1c; and - · · - · · - (for the design of the ejector presented on Figure 1d. Experimental data: •—for the design of the ejector presented on Figure 1a; ◆—for the design of the ejector presented on Figure 1b; ▲—for the design of the ejector presented on Figure 1c; and ■—for the design of the ejector presented on Figure 1d.

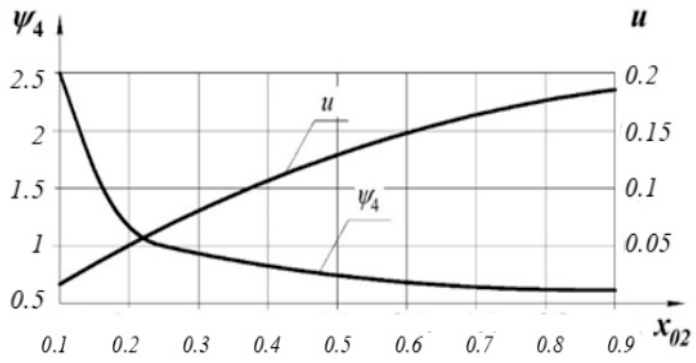


**Figure 8.** The degree of vapor overproduction and injection coefficient from mass vapor content in the secondary flow at the LVE inlet.

The experimental characteristics of the efficiency of the LVE and its corresponding vacuum unit are shown in Figure 9.

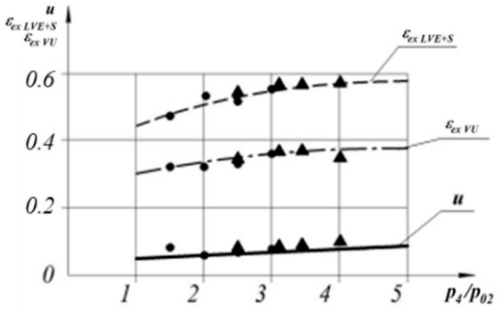


**Figure 9.** Dependence of achievable LVE performance indicators from the degree of pressure increase in the secondary flow.; Results of numerical research: ——— —*u*; —- —— $\varepsilon_{ex\ LVE+S}$; - · - · - —$\varepsilon_{ex\ VU}$. Experimental data: •—LVE with a cylindrical mixing chamber and ▲—LVE with a conical mixing chamber.

In this paper, we conducted an analysis using numerical and experimental studies on the effect of vapor overproduction in a liquid–vapor ejector on the efficiency of a vacuum unit. Based on our results, several significant advantages could be identified. First, using LVE, we gained the opportunity to implement a fundamentally new energy conversion cycle in which vapor generation occurred within the working process. It did not require additional equipment that would complicate the technological scheme of the installation. Secondly, using water as the working medium of a primary flow increased the efficiency and safety of the proposed unit.

The following features were found. For secondary flow pressure increases $p_4/p_{02} < 4$, LVE with a cylindrical mixing chamber and diffuser could be used; for $p_4/p_{02} > 4$, a conical mixing chamber and diffuser could be used. This was due to the time during which the mixing of the working media of primary and secondary flows and the completion of the processes of heat and mass transfer between the phases at different pressures and temperatures occurred.

This study determined how to choose the geometric parameters of the liquid–vapor ejector flow path, based on the initial parameters of the working media of primary and secondary flows. This made it possible to avoid off-design modes of operation of the ejector at its design stage. The experimental study results indicate correctness, making it possible to obtain such performance indicators.

The closest in design to the proposed type of apparatus are vapor jet ejectors with a water vapor working medium. However, they are multi-stage and have a total efficiency of 2–5%. They have low efficiency because, in one degree of the vapor jet ejector, a pressure difference of only two to three times can be created. In a liquid–vapor ejector, this difference is at a level of 8–10.

Limitations in applying this type of ejector are due to the vacuum values at the inlet to the secondary flow nozzle, which can be achieved at the level of 10–15 kPa. To obtain a lower value of this pressure, it is necessary to use fore vacuum pumps (booster or molecular).

The study carried out is a continuation of the research on the working process of liquid–vapor ejectors in the experimental direction described in [12–16]. The experimental data obtained in this work make it possible to determine the operating ranges of the liquid–vapor ejector as part of a vacuum unit, in which its efficiency will be maximized. This allows checking the mathematical model developed by the authors and, if necessary, introducing the appropriate correlation coefficients.

Further work could improve LVE workflow efficiency by profiling the diffuser part of the motive nozzle. However, it is necessary to improve the mathematical model that considers different nozzle geometry and conduct additional experimental studies.

## 4. Conclusions

As a result of our numerical and experimental studies, we found that in an ejector with a cylindrical or conical mixing chamber with a diffuser, the degree of vapor overproduction was $\psi_4$ = 1.4, and without a diffuser, $\psi_4$ = 2.3. The presence of a diffuser contributed to a greater degree of completion of the mixing process and obtained a two-phase vapor-droplet fine structure at the outlet of the ejector. The degree of vapor overproduction reached rational values at the level $\psi_4$= 1.10–1.25. The degree of steam overproduction was evaluated according to Formula (11), in which the values of mass steam content were taken from Figure 7.

As a result of the numerical study on the influence of mass steam content in a passive flow ($x_{02}$) on the steam overproduction in a mixed flow, we reached the following conclusion: at values of $x_{02} < 0.215$, the steam overproduction degree $\psi_4$ becomes less than 1. This leads to additional condensation of the passive flow steam (Figure 8).

As a result of the numerical studies, graphical dependence of vapor overproduction on the secondary flow parameters could be obtained. At the design stage, this can

determine the rational variant of the liquid–vapor ejector flow path with maximum efficiency indicators.

As a result of the exergy analysis of the liquid–vapor ejector with different flow path geometry, the efficiency indicators of the LVE with a cylindrical and conical chamber without a diffuser were obtained at the level $\varepsilon_{ex}$ = 30.5–33%, and with a diffuser at $\varepsilon_{ex}$ = 20–23.5%.

**Author Contributions:** Conceptualization, S.S. and J.M.; methodology, D.H. and V.P; software, I.P. and K.Ž.; validation, V.I., J.M. and K.Ž.; formal analysis, V.P.; investigation, S.S. and D.H.; resources, D.H.; data curation, I.P. and K.Ž.; writing—original draft preparation, S.S.; writing—review and editing, J.M. and V.I.; visualization, V.P.; supervision, S.S.; project administration, J.M.; funding acquisition, K.Ž. All authors have read and agreed to the published version of the manuscript.

**Funding:** This work was supported by the projects VEGA 1/0704/22, KEGA 055TUKE-4/2020 granted by the Ministry of Education, Science, Research and Sport of the Slovak Republic.

**Data Availability Statement:** Not applicable.

**Acknowledgments:** The scientific results have been partially obtained within the research project "Fulfillment of tasks of the perspective plan of development of a scientific direction "Technical sciences" Sumy State University," ordered by the Ministry of Education and Science of Ukraine (State Reg. No. 0121U112684). The research was partially supported by the Research and Educational Center for Industrial Engineering (Sumy State University) and the International Association for Technological Development and Innovations.

**Conflicts of Interest:** The authors declare no conflict of interest.

## References

1. Riaz, F.; Yam, F.Z.; Qyyum, M.A.; Shahzad, M.W.; Farooq, M.; Lee, P.S.; Lee, M. Direct Analytical Modeling for Optimal, On-Design Performance of Ejector for Simulating Heat-Driven Systems. *Energies* **2021**, *14*, 2819. [CrossRef]
2. Topal, H.I.; Tol, H.I.; Kopaç, M.; Arabkoohsar, A. Energy, exergy and economic investigation of operating temperature impacts on district heating systems: Transition from high to low-temperature networks. *Energy* **2022**, *251*, 123845. [CrossRef]
3. Besagni, G.; Cristiani, N.; Croci, L.; Guédon, G.R.; Inzoli, F. Multi-scale evaluation of ejector performances: The influence of refrigerants and ejector design. *Appl. Therm. Eng.* **2021**, *186*, 116502. [CrossRef]
4. Mahmoudian, J.; Mazzelli, F.; Milazzo, A.; Malpress, R.; Buttsworth, D. Experiments on water vapour condensation within supersonic nozzle flow generated by an impulse tunnel. *Int. J. Multiph. Flow* **2021**, *134*, 103473. [CrossRef]
5. Zhang, G.; Dykas, S.; Majkut, M.; Smołka, K.; Cai, X. Experimental and numerical research on the effect of the inlet steam superheat degree on the spontaneous condensation in the IWSEP nozzle. *Int. J. Heat Mass Transf.* **2021**, *165*, 120654. [CrossRef]
6. Bulinski, Z.; Smolka, J.; Fic, A.; Banasiak, K.; Nowak, A. A comparison of heterogenous and homogenous models of two-phase transonic compressible $CO_2$ flow through a heat pump ejector. *IOP Conf. Ser. Mater. Sci. Eng.* **2010**, *10*, 012019. Available online: https://iopscience.iop.org/article/10.1088/1757-899X/10/1/012019/pdf. (accessed on 20 January 2022). [CrossRef]
7. Zhang, G.; Zhang, X.; Wang, D.; Jin, Z.; Qin, X. Performance evaluation and operation optimization of the steam ejector based on modified model. *Appl. Therm. Eng.* **2019**, *163*, 114388. [CrossRef]
8. Smolka, J.; Bulinski, Z.; Fic, A.; Nowak, A.J.; Banasiak, K.; Hafner, A. A computational model of a transcritical R744 ejector based on a homogeneous real fluid approach. *Appl. Math. Model.* **2013**, *37*, 1208–1224. [CrossRef]
9. Dong, J.; Hu, Q.; Yu, M.; Han, Z.; Cui, W.; Liang, D.; Ma, H.; Pan, X. Numerical investigation on the influence of mixing chamber length on steam ejector performance. *Appl. Therm. Eng.* **2020**, *174*, 115204. [CrossRef]
10. Falsafioon, M.; Aidoun, Z.; Ameur, K. Numerical Investigation on the Effects of Internal Flow Structure on Ejector Performance. *J. Appl. Fluid Mech.* **2019**, *12*, 2003–2015. [CrossRef]
11. Sarevski, V.N.; Sarevski, M.N. Characteristics Of R718 Thermocompression Refrigerating/Heat Pump Systems With Two-Phase Ejectors. In Proceedings of the International Refrigeration and Air Conditioning Conference, West Lafayette, IN, USA, 16–19 July 2012; Available online: https://docs.lib.purdue.edu/iracc/1214/ (accessed on 10 December 2021).
12. Milazzo, A.; Rocchetti, A. Modelling of ejector chillers with steam and other working fluids. *Int. J. Refrig.* **2015**, *57*, 277–287. [CrossRef]
13. Grazzini, G.; Milazzo, A.; Mazzelli, F. *Ejector for Efficient Refrigeration*; Springer: Cham, Switzerland, 2018.
14. Sutthivirode, K.; Thongtip, T. Performance improvement of ejector refrigerator–based water chiller working with different mixing chamber profiles. *Alex. Eng. J.* **2021**, *60*, 3693–3707. [CrossRef]
15. Milazzo, A.; Mazzelli, F. Future perspectives in ejector refrigeration. *Appl. Therm. Eng.* **2017**, *121*, 344–350. [CrossRef]
16. Liao, Y.; Lucas, D. 3D CFD simulation of flashing flows in a converging-diverging nozzle. *Nucl. Eng. Des.* **2015**, *292*, 149–163. [CrossRef]

17. Butrymowicz, D.; Śmierciew, K.; Karwacki, J.; Gagan, J. Experimental investigations of low-temperature driven ejection refrigeration cycle operating with isobutane. *Int. J. Refrig.* **2014**, *39*, 196–209. [CrossRef]
18. Varga, S.; Lebre, P.S.; Oliveira, A.C. Readdressing working fluid selection with a view to designing a variable geometry ejector. *Int. J. Low Carbon Technol.* **2013**, *10*, 205–215. [CrossRef]
19. Hemidi, A.; Henry, F.; Leclaire, S.; Seynhaeve, J.M.; Bartosiewicz, Y. CFD analysis of a supersonic air ejector. Part I: Experimental validation of single-phase and two-phase operation. *Appl. Therm. Eng.* **2009**, *29*, 1523–1531. [CrossRef]
20. Colarossi, M.; Trask, N.; Schmidt, D.P.; Bergander, M.J. Multidimensional modeling of condensing two-phase ejector flow. *Int. J. Refrig.* **2012**, *35*, 290–299. [CrossRef]
21. Sharapov, S.; Prokopov, M.; Butrymowicz, D.; Kozin, V. Efficiency of a Vacuum Cooling System with Liquid-Vapor Ejector for Biodiesel Production. In Proceedings of the 10th International Conference on Compressors and Coolants, Bratislava, Slovakia, 13–15 January 2021. [CrossRef]
22. Sharapov, S.; Starchenko, M.; Protsenko, M.; Panchenko, V.; Kovtun, V. Improvement of the vacuum cooling system for biodiesel production. *J. Eng. Sci.* **2019**, *6*, F6–F11. [CrossRef]
23. Mastech M-838. Digital Multimeter User Guide. Available online: https://manuals.plus/m/176780fc3786754650afecf6e57df69976bf0ececc41d8d387f1b10bc9b203f0_optim.pdf&attachment_id=&dButton=true&pButton=true&oButton=false&sButton=true#zoom=auto&pagemode=none&_wpnonce=09183acb78 (accessed on 30 October 2022).
24. Chekh, O.; Sharapov, S.; Prokopov, M.; Kozin, V.; Butrymowicz, D. Cavitation in nozzle: The effect of pressure on the vapor content. In *Lecture Notes in Mechanical Engineering*; Springer: Cham, Switzerland, 2020; pp. 522–530. [CrossRef]
25. Morosuk, T.; Tsatsaronis, G. Advanced exergy-based methods used to understand and improve energy-conversion systems. *Energy* **2019**, *169*, 238–246. [CrossRef]
26. Morosuk, T.; Tsatsaronis, G. New approach to the exergy analysis of absorption refrigeration machines. *Energy* **2008**, *33*, 890–907. [CrossRef]
27. Wang, L.; Fu, P.; Yang, Z.; Lin, T.-E.; Yang, Y.; Tsatsaronis, G. Advanced Exergoeconomic Evaluation of Large-Scale Coal-Fired Power Plant. *J. Energy Eng.* **2020**, *146*, 04019032. [CrossRef]
28. Lishchenko, N.; Pitel', J.; Larshin, V. Online Monitoring of Surface Quality for Diagnostic Features in 3D Printing. *Machines* **2022**, *10*, 541. [CrossRef]